1, 93 (1976).
Petrie, C. J. S., *Elongational Flows*, Pitman, London (1979).
Phan-Thien, N., "A nonlinear network viscoelastic model," *J. Rheol.*, **22**, 259 (1978).
Spearot, T. A., and Metzner, A. B., "Isothermal spinning of molten polyethylenes," *Trans. Soc. Rheol.*, **16**, 495 (1972).
Ziabicki, A., *Fundamentals of Fibre formation*, J. Wiley, New York (1976).

Manuscript received June 29, 1981; revision received January 25, and accepted February 22, 1982.

Bed-Surface Contact Dynamics for Horizontal Tubes in Fluidized Beds

The local contact characteristics between the bed emulsion and the tube surface for horizontal tubes immersed in fluidized beds were investigated experimentally. The measurements indicated that the contact dynamics change significantly with circumferential position, gas flow rate, particle size and system pressure. From the experimental data, quantitative information on the local fluidization behavior were generated for use in heat transfer models.

RAVI CHANDRAN and J. C. CHEN

Institute of Thermo-Fluid Engineering & Science
Lehigh University
Bethlehem, PA 18015

SCOPE

Many applications of fluidized beds involve heat transfer to or from submerged tubes and tube bundles. Measurements of heat transfer between fluidized beds and horizontal tubes have been carried out by many investigators and both experimental data and correlations are reported in the literature (Saxena et al., 1978). However, as pointed out by Chandran et al. (1980), the conventional approach of relating heat transfer coefficients and operating parameters by means of empirical correlations seems to be inadequate.

A number of researchers have attempted the mechanistic approach and have developed semi-empirical relations for the heat transfer coefficient (Chandran, 1980). In order to examine the validity of the models that have been proposed, it is necessary to know the transient contact characteristics between the bed emulsion and the tube surface on a local basis. Until recently, a lack of such knowledge hampered the development and use of phenomenological models (Chen, 1976; Rooney and Harrison, 1976; Ozkaynak and Chen, 1980). From a design standpoint, there is a need for improved phenomenological understanding of the mechanisms and appropriate modeling of the transport processes. The objectives of this work were to generate the necessary information and to facilitate the development of a mechanistic model for the heat transfer process.

The experiments were performed in two different fluidized bed test facilities. Measurements were obtained in air-fluidized beds of glass beads for both a single tube and a ten-row bare tube bendle configuration. The capacitance probe technique, developed by Ozkaynak and Chen (1978) for contact measurements on a vertical tube, was used to investigate the dynamic characteristics of local fluidization behavior around horizontal tubes. Data were obtained for four different particle sizes (dia. ranging from 245 to 1580 μm), at three different system pressures (101.3, 202.6 and 405.3 kPa) and over a range of air flow rates (up to 12 times the minimum fluidization flow rate). The capacitance measurements were made at angular positions 90° apart around the circumference of the test tube in the case of single tube experiments and at 45° intervals in the case of multi-tube experiments.

CONCLUSIONS AND SIGNIFICANCE

The capacitance signals indicated distinctly different bed-surface contact characteristics at various angular positions around the tube. At low gas flow rates, the top surface of the tube remained covered by an essentially quiescent cap of densely packed particles with very long contact times and with no apparent displacement by passing bubbles. At the sides of the tube, a renewal type of contact with distinct periodic variations in the emulsion density was found. A different behavior was observed at the bottom of the tube. This segment was seen to encounter a relatively light-density emulsion with little fluctuation in the instantaneous density. A variation in the gas flow rate resulted in a marked change in the transient contact behavior. With an increase in the gas flow rate, the top of the tube experienced increasingly more effective scrubbing by passing bubbles and the stagnant cap was replaced by distinct "packets" of particles. The sides of the tube encountered more and more of the dilute void-phase, while the bottom portion of the tube experienced a renewal type of contact with the dense-phase packet contribution becoming important.

Quantitative information on the local fluidization characteristics were obtained by differentiating between a "dense phase" and a "lean phase" contact at the tube surface. The capacitance signals were processed to determine the values of the following parameters—root-square-average residence time of the dense phase, fractional contact time of the lean phase, and the average void fractions of the dense and the lean phases. The magnitude of these quantities were found to strongly depend upon circumferential position, gas flow rate, particle size and

Correspondence concerning this paper should be addressed to Ravi Chandran. He is now in the Department of Mechanical Engineering, Ohio University, Athens, OH 45701.
0001-1541-82-5353-0907-$2.00

system pressure.

The test results indicated that the dense phase contribution is significant for small particles and at low gas flow rates. The lean phase contribution seemed to become more important at high gas flow rates, for large particles and for elevated pressure operation. From the experimental data, empirical correlation curves for the fluidization parameters were generated for use in heat transfer models.

TEST APPARATUS AND EXPERIMENTAL METHOD

The experimental program was carried out in fluidized bed test facilities described elsewhere (Chandran et al., 1980; Chandran, 1980).

Local bed-surface contact dynamics were examined using fast response capacitance probes. Two test sections, one for use in the single tube experiments (Figure 1) and another for use in the multi-tube experiments, were designed and instrumented. The test tube shown in Figure 1 consisted of an aluminum solid cylinder flanked by two aluminum tubes. The solid cylinder contained two Lexan inserts, each of which in turn carried a pair of miniature capacitance electrodes implanted flush with the surface. For construction details, the reader is referred to Chandran (1980). The leads from the electrodes were connected to a circuit designed to sense capacitance changes of the order of a few pico-farads (Nixon, 1978). In principle, the circuit operated on an amplitude modulation scheme to yield a DC voltage output proportional to the capacitance sensed at the electrodes.

The single tube studies were carried out in fluidized beds of glass beads over a range of air flow rates (up to 12 times the minimum fluidization flow rate). Data were obtained for four different particle sizes ($245 \leq \bar{d}_p \leq 1580$ μm) and at pressures of 101.3, 202.6 and 405.3 kPa. The multi-tube experiments were performed with a medium size particle ($\bar{d}_p = 650$ μm) and at atmospheric pressure. Local fluidization dynamic measurements were obtained for a tube at two different positions within a ten-row bare tube bundle and over a range of air flow rates. Geometry of the tube bundle is shown in Chandran et al. (1980). The tubes were arranged in a staggered array with a horizontal pitch of 0.1016 m and a vertical pitch of 0.114 m. The tube bank was immersed in a 0.305 m square bed with the center of the bottom-row located 0.34 m above the distributor. The characteristics of the various test particles are furnished in Table 1. The mean particle diameter ($\bar{d}_p$) was computed on the usual basis of weight fractions (Kunii and Levenspiel, 1969; Botterill, 1975). The minimum fluidization velocity (U_{mf}) was determined experimentally by observation of pressure drop behavior. The value for the terminal velocity (U_t) was calculated by standard equations (Kunii and Levenspiel, 1969) for the smallest particle size in the bed.

In all tests, the static height of the (unfluidized) bed (H_s) was 0.46 m. In the case of single tube experiments, the center-line elevation of the tube above the distributor (H) was held constant at 0.23 m. The tube was 28.6 mm in diameter (D) and 189 mm in length. In tube bundle experiments, the instrumented tube was positioned at the center of row 1 (bottom-row) and row 3. The test tube was 286 mm long and had a diameter (D) of 31.8 mm. Capacitance data were obtained at 90° intervals in the case of single tube experiments and at 45° intervals in the case of multi-tube experiments.

EXPERIMENT RESULTS

As stated earlier, the capacitance probe was used to measure transient bed-surface contact behavior. The capacitance sensed by the probe is proportional to the dielectric constant of the fluidized medium local to the probe electrodes. The dielectric constant in turn depends on the local void fraction. Thus, a capacitance trace versus time can be directly related to the variations in local solids density at the tube surface. The measured capacitance signals were calibrated relative to an upper bound corresponding to the capacitance measured when the probe is immersed in a loosely packed static bed of particles, and a lower bound corresponding to the capacitance sensed when the probe is fully exposed to air. The intermediate capacitances measured in the fluidized conditions were normalized with respect to these two limits such that a value of 1.0 represents a state identical to a loosely packed static bed and a value of zero corresponds to that of a gas void. It is assumed that intermediate values are directly proportional to the local void fraction.

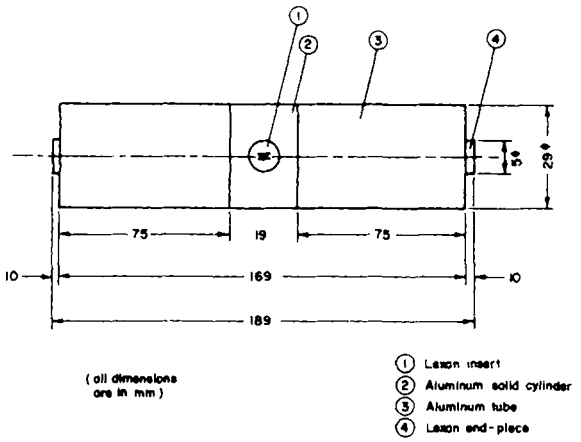

Figure 1. Capacitance test section used in single tube experiments.

For reasons stated in an earlier publication (Chandran et al., 1980), a normalized velocity parameter $(U_{sg} - U_{mf})/(U_t - U_{mf})$ is used to characterize the fluidization flow. The value of this velocity parameter (U_N) usually lies between 0 and 1. For fine powders, however, the value may exceed unity unless U_t is revised as the terminal velocity for the largest particle in the size range. The magnitude of U_N is indicated for all data shown in Figures 2 through 14.

Examples of typical capacitance signals obtained with an instrumented horizontal tube immersed in a fluidized bed of small particles ($\bar{d}_p = 245$ μm) are shown in Figures 2 and 3. These data were obtained for fluidization at atmospheric pressure. From Figure 2 it is seen that at low gas flow rates, the top surface of the tube remains covered by a stagnant cap of densely packed particles with very long contact times and no apparent displacement by passing bubbles. One would expect that in this regime heat transfer

TABLE 1. PROPERTIES OF TEST PARTICLES

Designation	Mean Size $\bar{d}_p$ (μm)	Size Range (μm)	U_{mf}(m/s) Pressure (kPa) 101.3	202.6	405.3	U_t(m/s) Pressure (kPa) 101.3	202.6	405.3	α_p
GT-1	125	105-149	0.024			0.83			
GT-2	245	210-297	0.051	0.051	0.050	1.66	1.32	1.07	0.35
GT-3	610	500-707	0.280	0.254	0.231	3.91	3.10	2.46	0.36
GT-5	950	707-1190	0.430	0.337	0.267	5.56	4.41	3.37	0.40
GT-6	1580	1410-1679	0.801		0.512	9.47		4.74	0.41
SG	650	595-707	0.31			4.6			0.36

Material: soda lime glass, density ρ_s: 2,480 kg/m^3; specific heat c_{ps}: 753 J/kg-K; thermal conductivity k_s: 0.89 W/m-K

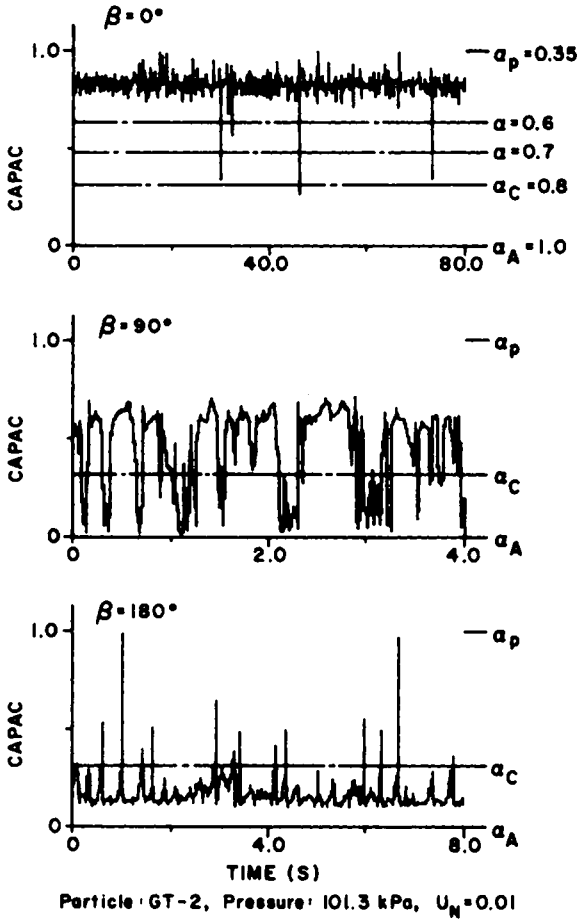

Particle: GT-2, Pressure: 101.3 kPa, U_N = 0.01

Figure 2. Capacitance traces at low gas flow rate.

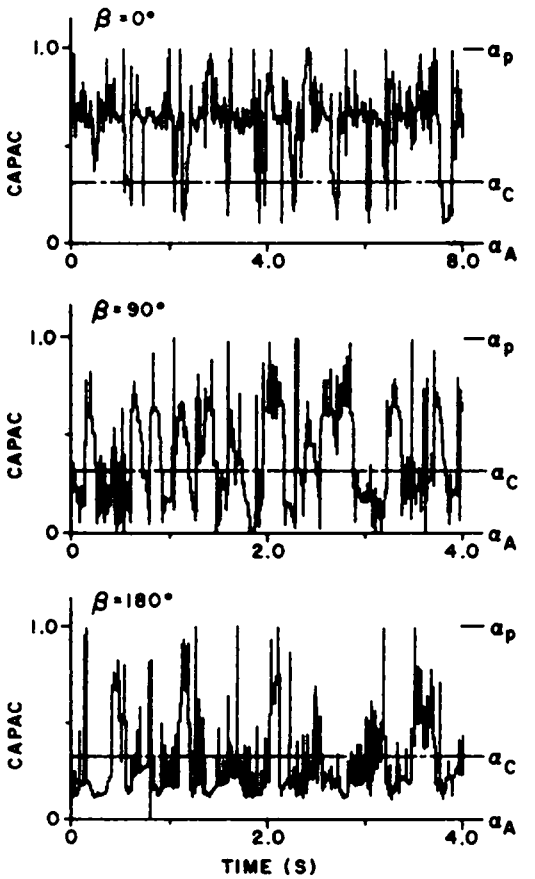

Particle: GT-2, Pressure: 101.3 kPa, U_N = 0.36

Figure 3. Capacitance traces at high gas flow rate.

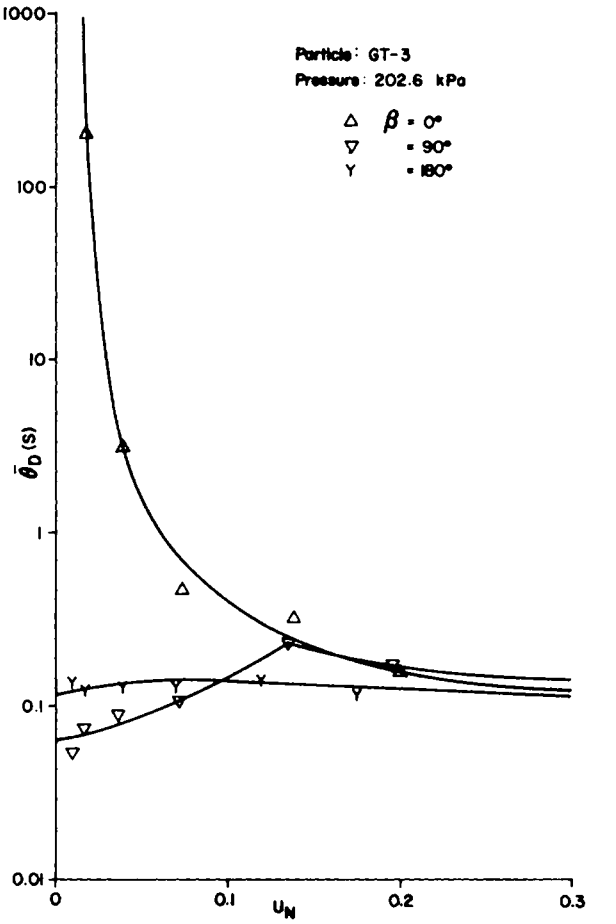

Figure 4. Effect of gas flow rate on dense phase root-square-average residence time around a single tube.

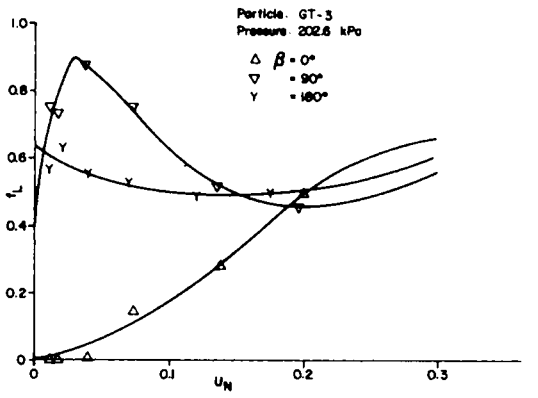

Figure 5. Effect of gas flow rate on fractional contact time of lean phase around a single tube.

would be dominated by conductive transfer with some enhancement due to ventilation flow of gas through the interstitial spaces. At the sides of the tube, a renewal type of contact with distinct periodic variations in the emulsion density is found. Another distinctly different behavior is observed at the bottom of the tube. The capacitance traces showed that this segment encountered a relatively light density emulsion with little fluctuation in the instantaneous density. One would expect that for this flow regime a dilute phase convective transport mechanism would be appropriate.

The qualitative behavior outlined above undergoes a change with the operating conditions, as can be seen, for instance in Figure 3. With an increase in the gas flow rate, the top of the tube experiences increasingly more effective scrubbing by passing bubbles until the stagnant cap is periodically replaced by packets of particles. The sides of the tube encounter more and more of lean phase,

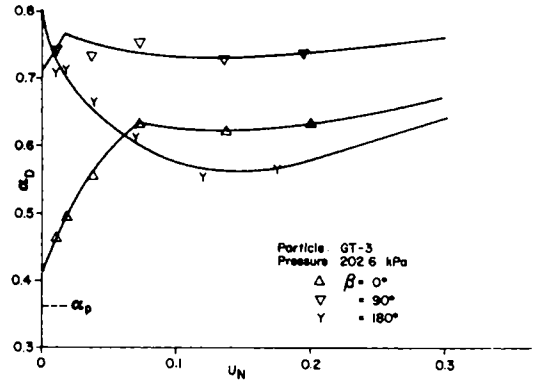

Figure 6. Effect of gas flow rate on dense phase void fraction around a single tube.

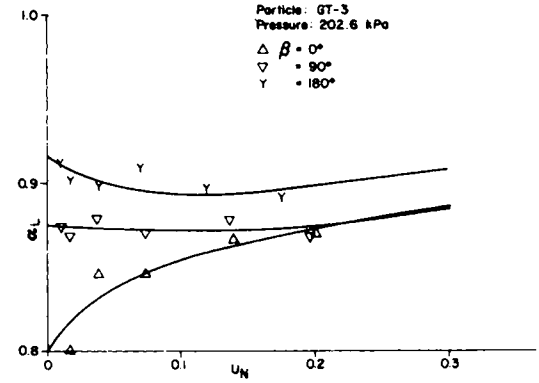

Figure 7. Effect of gas flow rate on lean phase void fraction around a single tube.

while the bottom portion of the tube experiences renewal type of contact with the dense phase contribution becoming important. These observations are consistent with those reported by previous investigators (Glass and Harrison, 1964; Botterill et al., 1966; Hager and Thomson, 1973; Rooney and Harrison, 1976).

In order to quantitatively describe the measured fluidization characteristics, it was decided to differentiate between a "dense phase" and a "lean phase" contact at the tube surface. This binary classification required that a suitable criterion be selected as a demarcation between the two phases. Three different criteria based on normalized capacitance signals of $\frac{1}{3}$, $\frac{1}{2}$ and $\frac{2}{3}$ (corresponding to average void fractions of 0.8, 0.7 and 0.6) were used in an attempt to find a suitable criterion. The first criterion ($\frac{1}{3}$; void fraction of 0.8) was found to give the most consistently meaningful interpretation of the contact characteristics. Besides, the observations of Zabrodsky et al. (1976) and Syromyatnikov et al. (1976) lend support to the choice of 0.8 as a cut-off value for the void fraction. At this value of bed voidage, the gas phase is said to become continuous, i.e., bubbles disappear according to Zabrodsky et al. (1976), while the flow is considered to be disperse by Syromyatnikov et al. (1976) for average bed void fractions exceeding 0.8. The details of the analysis of the capacitance signal are presented in Chandran (1980).

Using the procedure cited above, it was possible to determine the contact residence times (θ_D,θ_L) of the dense and the lean phases at the probe surface. For data obtained over sufficiently long sample times, it was also possible to compute the average void fractions of the dense and the lean phases (α_D,α_L). Likewise, the fraction of the total time exposed to each phase (f_L, 1-f_L) could be determined. In addition, the value of a quantity termed "root-square-average residence time of the dense phase" ($\bar{\theta}_D$) was calculated from the residence time (θ_D) data for each test run. This was done because $\bar{\theta}_D$ value is required as input to heat transfer models for predicting the local tube-bed heat transfer coefficient

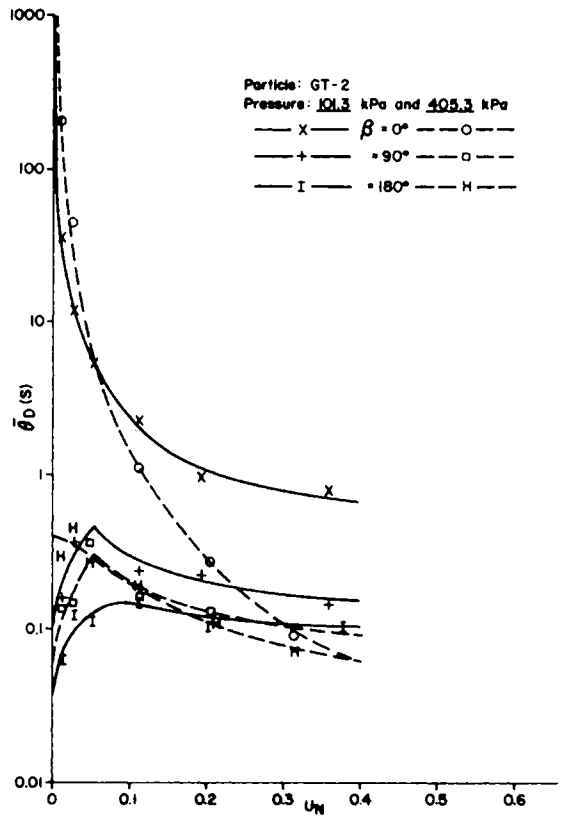

Figure 8. Effect of pressure on root-square-average residence time of dense phase for small particles.

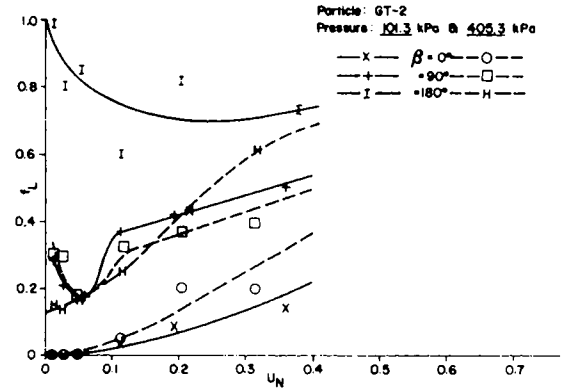

Figure 9. Effect of pressure on fractional contact time of lean phase for small particles.

(Mickley and Fairbanks, 1955; Ozkaynak and Chen, 1980; Chandran, 1980).

The fluidization data ($\bar{\theta}_D$, f_L, α_D, α_L) obtained in this investigation are tabulated in Chandran (1980).

Fluidization Data for a Single Tube

The plots of the fluidization parameters $\bar{\theta}_D$, f_L, α_D, and α_L as functions of the normalized velocity parameter (U_N), for three angular positions (β = 0°, 90° and 180°), are shown in Figures 4 through 7. The data shown were obtained with a medium size particle (GT-3) and at a system pressure of 202.6 kPa. From Figure 4, it is seen that the top of the tube (β = 0°) is initially in contact with a stagnant cap of densely packed particles. With an increase in gas flow rate beyond the minimum fluidization conditions, this cap is increasingly disturbed by bubbles passing nearby. Thus, renewal type mechanism gradually sets in and diminishes $\bar{\theta}_D$. At the top of the tube, f_L increases continuously from a value of zero at minimum fluidization, as shown in Figure 5. At the sides of the

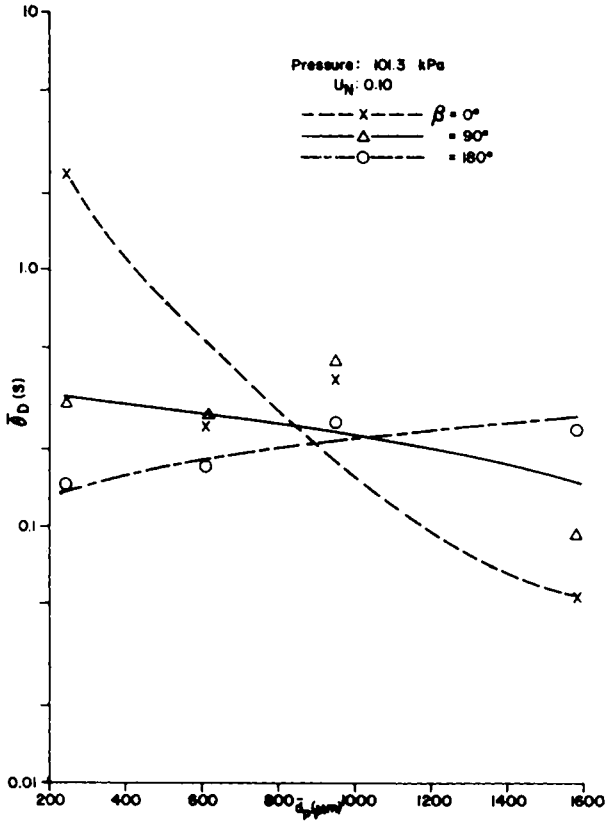

Figure 10. Effect of particle size on dense phase root-square-average residence time.

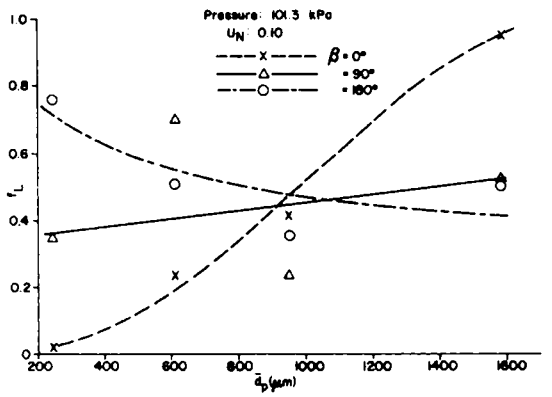

Figure 11. Effect of particle size on lean phase fractional contact time.

tube, initially with an increase in the gas flow rate, more lean phase comes into contact with the tube surface. This is probably due to increased bubble-activity. With further increase in the flow rate, f_L at first decreases due to enhanced particulate loading and particle circulation; but later with the onset of slug flow regime, f_L shows an increasing trend. The bottom of the tube exhibits a variation in f_L somewhat analogous to that at the sides of the tube, but the changes are less pronounced at this location.

Near minimum fluidization conditions, the cap at the top of the tube remains unfluidizied and so the dense-phase void fraction (α_D) has a value close to that of a packed bed (Figure 6). It increases rapidly at first and more slowly later with increments in U_N. The value of α_D at the sides of the tube is rather high (0.7–0.8), but it does not undergo any significant change over the flow rate range. With an increase in the gas flow rate, α_D decreases at the bottom of the tube from a value of 0.8 at minimum fluidization conditions. This is due to increased particulate loading and bubble-induced circulation. As the transition from bubbly to slug flow regime occurs, α_D at the bottom of the tube recovers and begins to increase

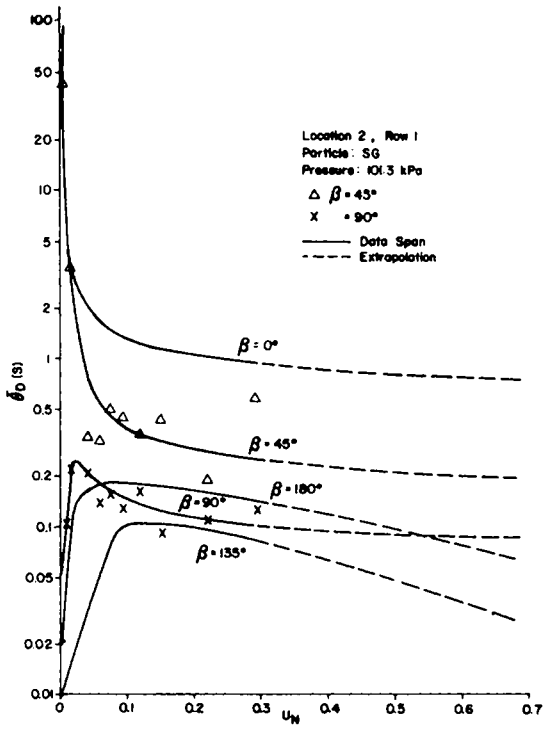

Figure 12. Dense phase root-square-average residence time for a tube in the bottom-row position within a tube bundle.

with flow rate. From Figure 7, it is seen that the lean phase void fraction (α_L) at the top of the tube has a value of 0.8 at U_{mf}; this is because no lean phase contact occurs at minimum fluidization conditions. α_L rises rapidly in the bubbly flow regime and increases more slowly with further increments in the gas flow rate. At the sides and bottom of the tube, the changes in α_L are less pronounced.

The effect of system pressure on the fluidization parameters ($\bar{\theta}_D$, f_L) is exhibited for a small size particle (GT-2) in Figures 8 and 9. From Figure 8, it is seen that $\bar{\theta}_D$ values at 405.3 kPa are generally lower than those at 101.3 kPa for all three angular positions (β = 0°, 90° and 180°), except at low values of U_N. The change in $\bar{\theta}_D$ due to pressure is especially pronounced for the top location (β = 0°), with higher residence times at low values of U_N and much lower contact times at other U_N values. At atmospheric pressure, the $\bar{\theta}_D$ values for the three angular positions are distinctly different from one another. But at 405.3 kPa, the residence time ($\bar{\theta}_D$) distribution tends to become uniform around the tube for reasonably large gas flow rates ($U_N > 0.25$). Figure 9 indicates that the values of f_L at the elevated pressure are higher for the top location (β = 0°) and generally lower for the side position (β = 90°), as compared to those at atmospheric pressure. But the bottom location (β = 180°) exhibits a radically different behavior. At atmospheric pressure, contact with the lean phase occurs most of the time; but at 405.3 kPa, more dense phase contact occurs initially and the fractional contact time of the lean phase increases with gas flow rate. A plot of α_D indicated that the void fraction is generally higher and the dense phase is more loosely packed at the higher pressure, for both the top and side positions (β = 0° and 90°); but the bottom location experiences contact with a considerably denser medium at the higher pressure, expecially at low gas flow rates. It was also found that the lean phase is less dilute and the values of α_L are somewhat lower at 405.3 kPa, in contrast with the results at atmospheric pressure, for all three angular positions. Thus it seems that in the case of small particles (GT-2), the contributions of both the dense phase and the lean phase mechanisms to heat transfer increase with pressure. The dense phase contribution is enhanced by shorter contact times, while the increased lean phase contribution results primarily from the gas density scaling effect. This serves to provide an explanation for the observed increase in heat transfer coefficients with system pressure (Chandran et al., 1980).

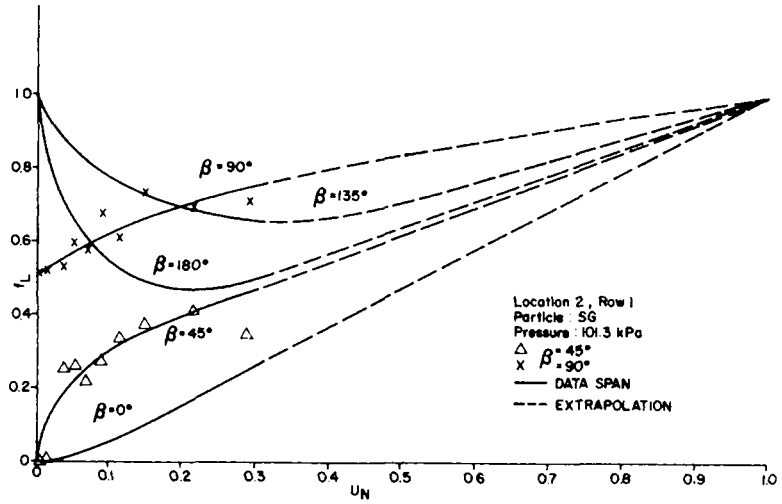

Figure 13. Lean phase fractional contact time for a tube in the bottom-row position within a tube bundle.

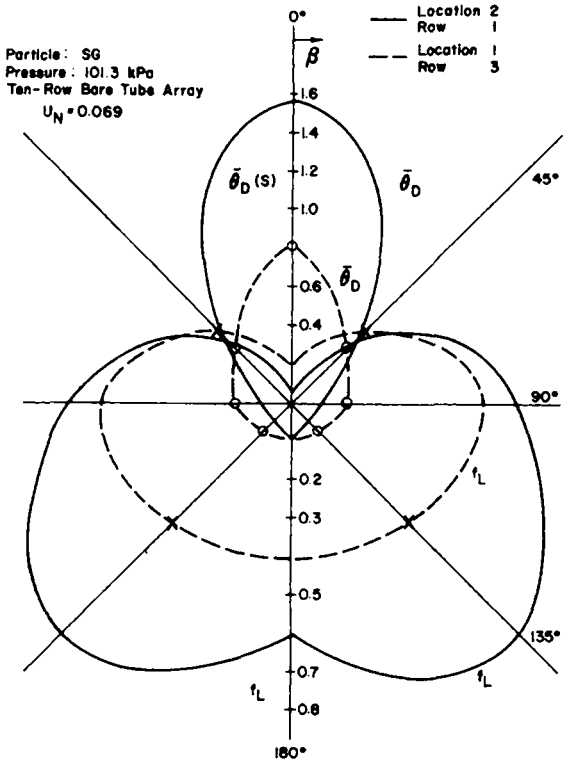

Figure 14. Local fluidization parameters for a test tube at two different locations within a tube bundle.

From the test results for large particles (GT-6), it was apparent that the fluidization parameters are affected only to a small extent by pressure. The residence time plot indicated that $\bar{\theta}_D$ values are slightly lower at 405.3 kPa, for all three angular positions. It was found that more lean phase contact with the tube surface occurs (larger f_L values) at the higher pressure, for the top and bottom locations; very little change in f_L occurs at the side position. Plots for α_D and α_L showed that pressure has little effect on the dense phase and the lean phase void fractions over the flow rate range tested. Thus it seems that in the case of large particles (GT-6), the improvement seen in the local heat transfer coefficients with pressure (Chandran et al., 1980), occurs mainly due to the increment in the lean phase contribution. The enhanced lean phase transfer, in turn, is attributable to the gas density scaling effect. Hence, for large particles convective transport becomes more and more important with an increase in the operating pressure.

The effect of particle size ($\bar{d}_p$) on the fluidization parameters at atmospheric pressure is shown in Figures 10 and 11. Each plot corresponds to a velocity parameter (U_N) value of 0.10. Figure 10 indicates that particle size has a considerable influence on $\bar{\theta}_D$ for the top location ($\beta = 0°$). Surface renewal seems to occur more often at the top of the tube, for large particles rather than for small particles. This serves to explain the high degree of nonuniformity observed in the local heat transfer coefficient distribution around the tube, for small particles at low gas flow rates (Chandran et al., 1980). The values of $\bar{\theta}_D$ for the side and bottom locations are little affected by particle size. The curve for the side position exhibits a decreasing trend, while that for the bottom location shows a rising characteristic. It is seen from Figure 11 that $\bar{d}_p$ has a sizable influence on f_L. For the top location, f_L steadily increases from almost 0 to 1 as the particles are changed from GT-2 to GT-6. The curves for the side and bottom positions exhibit increasing and decreasing trends respectively. Thus with an increase in particle size, the fractional contact time of the lean phase (f_L) increases for the top and side positions while dense phase fractional contact time ($1-f_L$) increases for bottom location. A plot of α_D indicated that with an increase in $\bar{d}_p$, the dense phase that comes into contact with the top and side positions is more dilute or loosely-packed; and the medium that contacts the bottom location is more dense. But the lean phase void fraction (α_L) showed an increasing trend with particle size for all three angular positions. In summary, the values of the fluidization parameters ($\bar{\theta}_D$, f_l, α_D, α_L) are altered by particle size ($\bar{d}_p$); the nature and extent of the variation, however, depends on the angular position (β).

Fluidization Results for Tube Bundle

Fluidization data were obtained by placing an instrumented tube at two different positions within a ten-row bare tube bundle. Measurements were obtained with glass particles SG (Table 1) at atmospheric pressure.

The plots of $\bar{\theta}_D$ and f_L as functions of normalized velocity (U_N), with angular position β as a parameter, are shown in Figures 12 and 13. The data pertain to location 2 (row 1 or bottom-row) in the tube array. For clarity, only the data points that correspond to the angular positions of $\beta = 45°$ and 90° are exhibited. In all cases, the curves drawn through the data points over the data span have been shown as solid lines and in the extrapolated region as dotted lines.

From Figure 12, it is apparent that just beyond minimum fluidization conditions, the top portion of the tube ($\beta = 0°$ and 45°) remains covered by a stagnant cap of densely packed particles. With an increase in gas flow rate, this cap is more increasingly disturbed by passing bubbles. Consequently, $\bar{\theta}_D$ diminishes and the renewal type mechanism gradually sets in. The bottom segment of the tube ($\beta = 135°$ and 180°) initially is in contact with a gas void and $\bar{\theta}_D$ evidently is zero. With a rise in gas flow, increased particulate loading and circulation occurs. The dense phase contribution and $\bar{\theta}_D$ increase steeply before slowly declining at very high ve-

locities. At the sides of the tube, the renewal mechanism controls and $\bar{\theta}_D$ does not undergo any significant change over most of the flow range.

For $\beta = 0°$, 45° and 90°, f_L increases steadily from 0 to 1, as can be seen in Figure 13. At the bottom of the tube, near minimum fluidization velocity, only the lean phase is present and hence f_L has a value of unity. With an increase in the gas flow rate, more dense phase comes into contact with the tube surface due to bubble-induced circulation and decreases f_L; but with the onset of slug flow regime, f_L starts to increase and approaches unity.

The plots for α_D and α_L indicated the following trends: Near minimum fluidization conditions, the cap at the top of the tube ($\beta = 0°$ and 45°) remains unfluidized and so the dense phase void fraction (α_D) has a value close to that of a packed bed. It approaches a value of 0.8—the reference level for cut-off between the phases—as the U_N parameter approaches unity. α_D decreases at the bottom of the tube with an increase in the gas flow rate from the minimum fluidization conditions, due to increased particulate loading and particulate circulation. As the transition from bubbly to slug flow regime occurs, α_D at the bottom of the tube recovers and slowly approaches 0.8 at very high flow rates.

There is no lean phase present at the top of the tube at U_{mf} and so the void fraction α_L has a value of 0.8. With an increase in gas flow rate, α_L rises rapidly in the bubbly flow regime. At the sides and bottom of the tube, the change in α_L is not pronounced. But in all the cases, α_L approaches unity as the U_N parameter tends to 1, as required by physical considerations.

The effect of tube location on the parameters $\bar{\theta}_D$ and f_L, at a U_N value of 0.069, is shown in Figure 14. It is seen that for the top portion of the tube at location 1, the $\bar{\theta}_D$ values are lower and the f_L values somewhat higher than those for the tube at location 2. This indicates more effective scrubbing by passing bubbles and in turn more frequent surface renewal at the inner-row position. At the sides and bottom of the tube, $\bar{\theta}_D$ values are slightly higher and the f_L values are lower for location 1 as compared to those for location 2. This denotes increased dense phase contact with the tube at the inner-row position. From the test results for void fraction it was seen that the dense phase that comes into contact with the bottom-row tube is more dilute or loosely-packed than the dense medium that contacts the inner-row tube. α_L values were slightly higher for the tube at location 2 than those for the tube at location 1.

The fluidization data for a test tube at two locations within the bundle were compared with those obtained for a single tube (GT-3, 101.3 kPa). For a fixed value of the flow-rate parameter (U_N), the values of $\bar{\theta}_D$ and f_L for the single tube were closer to those for the tube at the inner-row position (location 1 in the bundle). The values of the void fractions α_D and α_L for the single tube, however, were closer to those for the bottom-row tube (location 2 in the bundle).

SUMMARY

Capacitance probe measurements on the surface of horizontal tubes showed that local bed-surface contact dynamics depend strongly upon gas flow rate and circumferential position. In general, it was observed that at flow rates close to minimum fluidization conditions, the top portion of the tube remains covered by a dense emulsion, the sides of the tube experience a renewal type of contact with alternating voids and dense packets, and the bottom portion of the tube tends to be continuously washed by a gaseous medium with some entrained particles. These circumferential differences were seen to diminish with increasing flow rate.

From the test results, the dense phase void fraction was found to vary from 0.4 to 0.8, while the lean phase void fraction was found to range from 0.8 to 1.0. In contrast, the values of the dense phase residence time and the fractional contact time of the lean phase were observed to vary significantly with gas flow rate and circumferential position. The data indicated that the contact characteristics are complex in the bubbly flow regime but become more ordered in the slug and turbulent flow regimes, as the flow rate is increased. In addition, the magnitude of the fluidization parameters were affected by both particle size and system pressure.

Capacitance data obtained with an instrumented tube at two different locations within a tube bundle indicated dense phase contact to occur more often for a tube at the inner-row position than for a tube in the bottom-row of the bundle.

With a knowledge of the fluidization characteristics around horizontal tubes, a phenomenological model for the local heat transfer coefficient has been developed based on combined dense phase and lean phase transfer mechanisms. This model will be presented in a subsequent paper.

ACKNOWLEDGMENT

The authors wish to express their gratitude to T. L. Nixon for developing the probe electronics and express their appreciation for the help provided by the staff in the ME and Mech. Dept. of Lehigh University. The authors are grateful for the support of, and advise given to, this investigation by the Corporate Research and Development Center of General Electric Co.

NOTATION

D = tube diameter
$\bar{d}_p$ = mean particle diameter
f_L = fraction of the total time lean phase is in contact with the tube surface
H = center-line elevation of instrumented tube above the distributor
H_s = static bed height
P = absolute pressure
U_{mf} = superficial gas velocity at minimum fluidization condition
U_N = normalized velocity parameter or reduced velocity, $(U_{sg} - U_{mf})/(U_t - U_{mf})$
U_{sg} = superficial gas velocity
U_t = particle terminal or free-fall velocity

Greek Symbols

α = void fraction
α_c = void fraction cut-off value for differentiating between dense phase and lean phase contact with the tube surface
β = angular position around the circumference of tube, measured from the top of the tube
θ = residence time
θ_D = dense phase root-square-average residence time

Subscripts

A = air
D = dense phase
L = lean phase
mf = minimum fluidization state
P = packed state

LITERATURE CITED

Botterill, J. S. M., J. S. George, and H. Besford, "Bubble Chains in Gas Fluidized Beds," *Chem. Eng. Prog. Symp. Ser.*, **62**, (62), 7 (1966).

Botterill, J. S. M., *Fluid-Bed Heat Transfer*, Academic Press, New York (1975).

Chandran, R., J. C. Chen, and F. W. Staub, "Local Heat Transfer Coefficients around Horizontal Tubes in Fluidized Beds," *J. Heat Transfer* (Trans. ASME), **102**, 152 (1980).

Chandran, R., "Local Heat Transfer and Fluidization Dynamics around Horizontal Tubes in Fluidized Beds," Ph.D. Dissertation, Lehigh University, Bethlehem, PA (1980).

Chen, J. C., "Heat Transfer to Tubes in Fluidized Beds," ASME Paper 76-HT-75, ASME-AIChE Heat Transfer Conf., St. Louis, MO (1976).
Glass, D. H., and D. Harrison, "Flow Patterns Near a Solid Obstacle in a Fluidized Bed," *Chem. Eng. Sci.*, **19**, 1001 (1964).
Hager, W. R., and W. J. Thomson, "Bubble Behavior around Immersed Tubes in a Fluidized Bed," *AIChE Symp. Ser.*, **69**, (128), 68 (1973).
Kunii, D., and O. Levenspiel, *Fluidization Engineering*, John Wiley and Sons, New York (1969).
Mickley, H. S., and D. F. Fairbanks, "Mechanism of Heat Transfer to Fluidized Beds," *AIChE J.*, **1**, 374 (1955).
Nixon, T. L., "Circuit Design for Capacitance Probes," Instrumentation Lab., ME and Mech Dept., Lehigh University, Bethlehem, PA (1978).
Ozkaynak, T. F., and J. C. Chen, "Average Residence Times of Emulsion and Void Phases at the Surface of Heat Transfer Tubes in Fluidized Beds," *AIChE Symp. Ser.*, **74**, (174), 334 (1978).
Ozkaynak, T. F., and J. C. Chen, "Emulsion Phase Residence Time and Its Use in Heat Transfer Models in Fluidized Beds," *AIChE J.*, **26**, (4), 544 (1980).
Rooney, N. M., and D. Harrison, "Flow Patterns Near Horizontal Tubes in a Gas-Fluidized Bed," *Fluidization Technology*, **II**, ed., D. L. Keairns, Hemisphere Publishing Corp., Washington, 3 (1976).
Saxena, S. C., N. S. Grewal, J. D. Gabor, S. S. Zabrodsky, and D. M. Galershtein, "Heat Transfer Between a Gas Fluidized Bed and Immersed Tubes," *Adv. Heat Trans.*, **14**, 149 (1978).
Syromyatnikov, N. I., V. M. Kulikov, V. S. Nosov, and V. N. Korolev, "The Instantaneous Local Rate of External Heat Transfer in an Inhomogeneous Fluidized Bed," *Heat Transfer—Sov. Res.*, **8**, (5), 42 (1976).
Zabrodsky, S. S., N. V. Antonishin, and A. L. Parnas, "On Fluidized Bed-to-Surface Heat Transfer," *Can. J. Chem. Eng.*, **54**, 52 (1976).

Manuscript received February 2, 1981; revision received October 26, and accepted November 5, 1981.

Experimental Measurement of the Thermal Stability Criteria for the Low Pressure Methanol Synthesis

The mathematical basis was derived for the experimental measurement of the "Slope Condition" and of the "Dynamic Condition" of the thermal stability criteria in a laboratory-scale internal recycle reactor. This work also resulted in clearer interpretations and simpler expressions for the two stability criteria. The method was experimentally demonstrated on the example of the low pressure methanol synthesis. Only seven experiments were needed to evaluate the stability criteria of this reaction for which the kinetics is unknown.

J. M. BERTY, J. P. LENCZYK and S. M. SHAH

Department of Chemical Engineering
The University of Akron
Akron, OH 44325

SCOPE

The objective of this study was to develop an experimental method for the measurement of the thermal stability criteria. These are needed for the design of thermally stable commercial reactors, including auto-thermally operated converters. The knowledge of these criteria is needed already in the early conceptual design stage of a new process, sometimes even before a detailed kinetic model can be developed.

The second objective of this work was to show that even in the absence of knowledge on the kinetics of the reaction, the basic parameters for the stability criteria can be evaluated from a few experiments. These can be made in an internal recycle reactor operating as a CSTR at, or close to, the operating conditions of anticipated commercial process. The results can be used in the design of cooled tubular, or adiabatic production reactors and the results are not dependent on any assumptions made on the kinetics. In the opposite case, when kinetics is known, these experiments can serve as checks that are independent of the assumptions made in the kinetic study.

Historically, the original work of Liljenroth (1918), Damköhler (1937), and Wagner (1945) went unnoticed while the papers of Wilson (1946) and Frank-Kamenetskii (1939, 1961) had the first impact on the industry, and Van Heerden's (1953, 1958) papers started an avalanche of theoretical investigations. In the papers of both Wilson and Frank-Kamenetskii, the thermal stability criterion is expressed as a maximum permissible temperature difference for heat removal, that is a unique function of the energy of activation. An internal report from Union Carbide by Perkins in 1938 revealed the existence of a limiting maximum temperature difference for thermally stable operation that can be calculated from the energy of activation. These are simplified functions, and express conservative estimates built on the assumption of a zero order reaction rate. Frank-Kamenetskii recognized this and modified it on the basis of geometric arguments. Although these estimates were too simple and too conservative, they served the industry better than most of the work that followed. Theoretically better criteria developed later are elegant mathematical solutions of variations of the same problem. Generalization and basic understanding has not advanced much and Luss (1980) expressed the need for these.

Schmitz (1975) in his extensive review on the subject of stability estimated that only about 40% of the published papers in the last two decades were referenced on his list that counts close to 300 papers. He estimates also that references from areas other than chemical reactions amounted to an even smaller fraction. In spite of this, it is most likely that he caught all of the approximately 45 experimental papers. Of these, only eight were made on chemical systems that could have some industrial importance. The rest of the experiments were made on model reactions, like the oxidation of H_2, to test some theoretical

Correspondence concerning this paper should be directed to J. M. Berty.
J. P. Lenczyk is at the B & D Center of the B. F. Goodrich Co., Brecksville, OH 44141.
S. M. Shah is at Div. of Water, Dept. of Nat. Res. and Env. Prot. of the State of Kentucky, Frankfort, KY 40601.
0001-1541-82-4468-0914-$2.00.